2×20 Gbps - 40 GHz OFDM Ro-FSO transmission with mode division multiplexing

A. Amphawan
angela@uum.edu.my
InterNetWorks Research Laboratory, School of Computing, Universiti Utara Malaysia, Kedah, Malaysia
Research Laboratory of Electronics, Massachusetts Institute of Technology, Cambridge, USA

S. Chaudhary
InterNetWorks Research Laboratory, School of Computing, Universiti Utara Malaysia, Kedah, Malaysia

V. W. S. Chan
Research Laboratory of Electronics, Massachusetts Institute of Technology, Cambridge, USA

Radio-over-Free-Space-Optics (Ro-FSO) is a promising technology for future wireless networks. In this work, we have designed a hybrid orthogonal frequency division multiplexing (OFDM) Ro-FSO system for transmission of two independent channels by mode division multiplexing. Two independent 40 GHz radio signals are optically modulated at 20Gbps by mode division multiplexing of two laser modes LG00 and LG10 and transmitted over a free-space link of 20 km to 100 km. The performance of proposed Ro-FSO system is also evaluated under the effect of strong atmospheric turbulences.
[DOI: http://dx.doi.org/10.2971/jeos.2014.14041]

Keywords: Mode division multiplexing, LG modes, Ro-FSO, atmospheric turbulences

1 INTRODUCTION

The escalating bandwidth demand for future pervasive wireless networks has led to the rise of Radio-over-Free-Space-Optics (Ro-FSO) which has advantageous features of both radio-over-fiber (RoF) and free-space-optics (FSO). The limited availability of radio frequency (RF) spectrum has challenged the International Telecommunication Union (ITU) in the distribution of the available spectrum among mobile operators [1]. The main benefits of RoF technology includes the ability to distribute RF signals at large bandwidth using an optical carrier at low attenuation losses, immunity to radio frequency interference and low power consumption [2]. RoF technology has been the driver for sharing expensive equipment responsible for processes such as coding & decoding, multiplexing & de-multiplexing, frequency up-down conversion from the centralized station to all base stations. This results in reduction in cost and system complexity. On the other hand, FSO utilizes the atmosphere for transmission of signals instead of fiber optics. The transmitting lens projects the light signal in the atmosphere towards the receiving lens. FSO has become very attractive as an alternative for radio base stations and optical fiber given its ability to cope with high bandwidth without expensive cabling, license-free operation and imperceptibility to interference due to line-of-sight transmission [3, 4].

A Ro-FSO system harnesses the assets of both RoF and FSO technologies by incorporating the high bandwidth of optical networks and the mobility of wireless networks. Much attention has been given to increasing the speed of Ro-FSO systems. In an experiment [5], a wavelength division multiplexing scheme (WDM) is deployed to transmit the multiple RF signals over free space. In an experiment [6], dense wavelength division multiplexing (DWDM) scheme is employed to carry the RF signals over a free space link having a span of 1 km. In another experiment [7], the performance of OFDM is investigated in a Ro-FSO system for short range applications. Apart from wavelength multiplexing, for further increase in the capacity of Ro-FSO systems, mode division multiplexing (MDM) may be used as another multiplexing dimension. MDM allows transmission of a number of channels on different modes generated by various mechanisms such as by means of a spatial light modulator (SLM) [8, 9], optical signal processing [10]−[12], photonic crystal fiber [13] and single mode fiber [14]. MDM of various orthogonal modes has been demonstrated for FSO. In [15], the performance of MDM of three orbital angular momentum (OAM) modes of l = 1, 3, 5 from two reflective SLMs encoding spiral phase patterns through free-space was evaluated under emulated atmospheric turbulence by characterizing the effects of turbulence on crosstalk and system penalty. In [16], MDM of four 42.8 Gb/s OAM modes (l = +4, -8, +8, +16) was demonstrated by spiral phase masks encoded on SLMs, each polarization multiplexed on two polarizations using polarizing beam splitters for carrying 16-level quadrature amplitude modulation (QAM) signals, thus realizing a capacity of 42.8×4×4×2 Gbit/s. In another three-dimensional multiplexing experiment [17], quadrature phase shift keying (QPSK) signals were transmitted on 12 OAM beams generated using a phase mask on the first SLM to generate OAM beams with l = ±4, ±10, ±16 and another phase plate on the second SLM to generate OAM beams with l = ±1, ±7, ±13 and ±19, each transmitted on 2 polarizations and 42 spaced wavelengths, achieving 1008 data channels at an aggregate rate of 100.8 Tb/s. In [18], the Laguerre-Gaussian correlated Schell-model (LGCSM) vortex beam was

Received February 05, 2014; resubmitted June 22, 2014; revised ms. received July 15, 2014; published September 26, 2014 ISSN 1990-2573

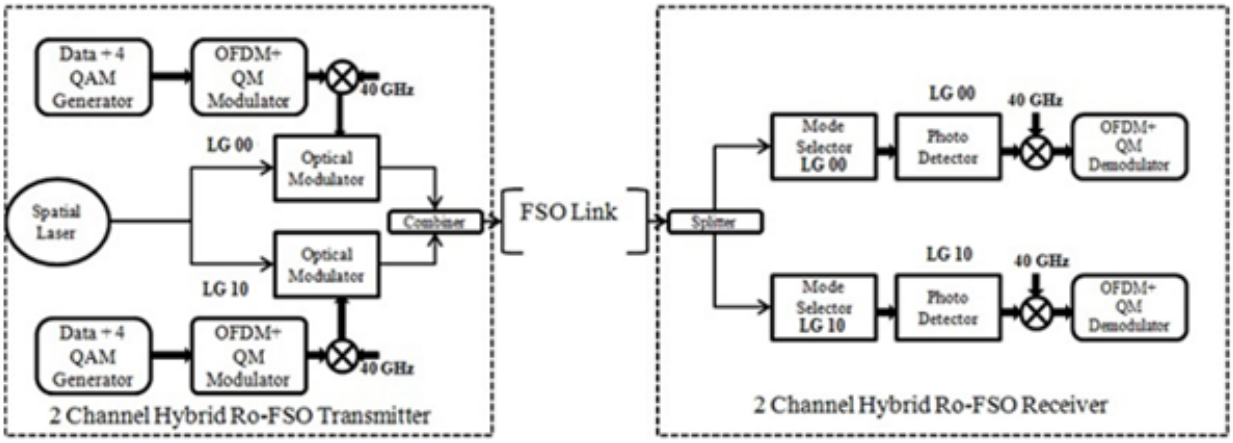

FIG. 1 Proposed 2 ×20 Gbps Hybrid Ro-FSO Transmission System.

generated through conversion of a LGCSM beam with the help of a spiral phase plate encoded on a SLM and the beam profile in the far-field was shaped by varying its initial spatial coherence. In [19], orbital angular multiplexing was used for transportation of 2 Tb/s data on 25 wavelengths. In [20], a silicon-on-insulator (SOI) wafer was fabricated for free-space MDM coherent optical transmission using five OAM modes (l = 0, ±1, ±2) for binary and quadrature phase shift keying. In [21], it is demonstrated that several partially overlapping fundamental Gaussian beams that are mutually incoherent are effective for reducing scintillations in FSO links. Numerical analyses have also been investigated on various types of mode profiles for FSO. In [22], expressions for average intensity and effective size of Laguerre-Gaussian and Bessel-Gaussian Schell-model beams are derived under atmospheric turbulence with detailed analyses on the effects of the atmospheric turbulence and source coherence on the intensity profile and beam profile. In [23], analytical expressions for the cross-spectral density and second-order moments of Wigner distribution function of a Laguerre-Gaussian Schell-model (LGSM) beam in turbulent atmosphere are derived to investigate statistical properties such as the degree of coherence and the propagation factor. The analysis shows that a LGSM beam with larger mode order n is less affected by turbulence. In [24], the expression of spectral density of cosine-Gaussian-correlated Schell-model (CGSM) beams diffracted by an aperture is derived to investigate the changes in the spectral density distribution of CGSM beams through propagation.

Although extensive experimental and numerical analyses have been undertaken for MDM of various modes in FSO, thus far, not much attention has been given to MDM in Ro-FSO systems. In this paper, we present for the first time radio QAM-OFDM 2 ×20 Gbps 40 GHz Ro-FSO system by with Laguerre-Gaussian MDM scheme for long haul communication. The originality of this study is in the combination of radio QAM-OFDM and optical MDM in FSO, in addition to the mode multiplexer-demultiplexer design. The objective of this study is to evaluate the performance of the combination of radio QAM-OFDM and optical MDM through FSO using a new mode multiplexer-demultiplexer design. In terms of scientific merits, our results demonstrate that the combination of radio OFDM and optical MDM is capable of extending the FSO distance to 90 km under clear weather conditions. The performance of such Ro-FSO system is also reported under the effect of scintillations. The rest of the paper is organized as follows: Section 2 describes the system description; Section 3 describes the result and discussion followed by the Section 4 in which the conclusion is presented.

2 SYSTEM DESIGN

A schematic diagram of proposed hybrid high speed Ro-FSO transmission system is shown in Figure 1. In the proposed system, two Laguerre-Gaussian (LG) modes LG00 and LG10 were multiplexed through free-space. The transverse spatial profile of the LG mode in the source plane $z = 0$ is described by [25]:

$$\psi_{m,n}(r,0,\theta) = \left(\frac{r}{\omega_0}\right)^m L_n^m\left(\frac{r^2}{\omega_0^2}\right) exp(jm\theta) \qquad (1)$$

where L_n^m is the associated Laguerre polynomial, n and m represent the azimuthal and radial mode numbers, $r = (x^2 + y^2)^{1/2}$ is the radius of curvature, $\theta = tan^{-1}(y/x)$ and w_0 is the beam waist width of the fundamental Gaussian mode. Linearly polarized transverse electric field of the two LG modes to be transmitted were experimentally generated using a transmissive binary amplitude SLM, three lenses and a pinhole, based on [26]. The construction of the mode transmitter is shown in Figure 2. A binary grating for the LG modes was encoded on a spatial light modulator. A collimated beam from the laser was expanded and directed through the spatial light modulator. The binary hologram from the spatial light modulator was Fourier transformed by the first lens of focal length 300 mm. A 0.2 mm pinhole was then used to retrieve the first diffraction order which was then scaled by the second lens of focal length 100 mm and third lens of focal length 3 mm. The modal fields were then concentrically combined. The amplitude and phase of the generated modal electric field were measured and inserted into the OptiSystem™ software. The electric field intensities of the generated LG00 and LG10 modes are given in Figure 3(a) and Figure 3(b) respectively. The electric field intensity of the combination of both modes are shown in Figure 3(c). The modulation and wave propagation were modelled in MATLAB and

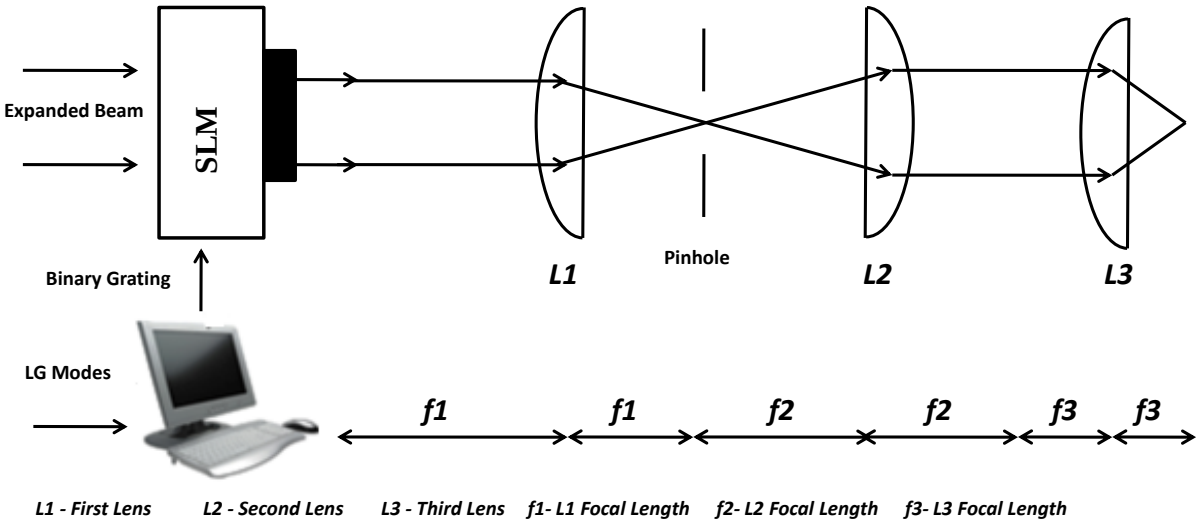

FIG. 2 LG mode wavefront multiplexer.

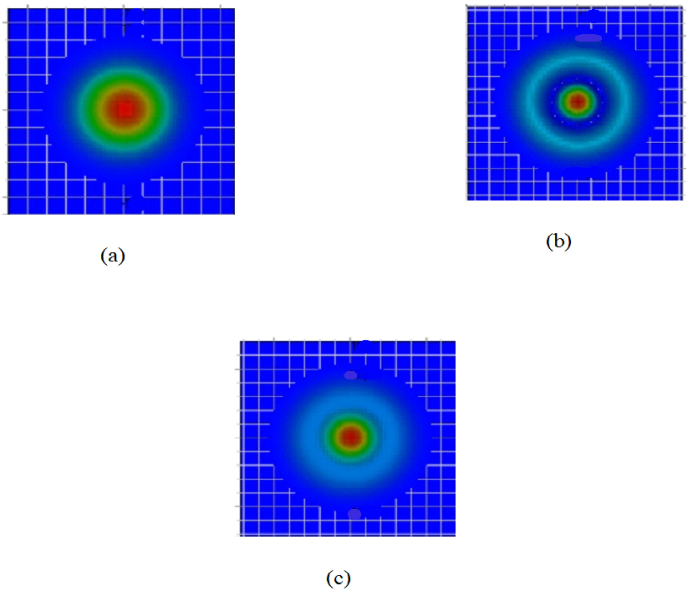

FIG. 3 Intensity fields of generated LG modes (a) LG00 (b) LG10 (c) LG00 + LG10.

Parameters	Value
Transmitter Aperture Diameter	3 μm
Receiver Aperture Diameter	10 cm
Beam Divergence	2 μrad
Spatial CW Laser Power	0 dBm
Spatial CW Laser Linewidth	10 MHz

TABLE 1 System Parameters

Optisystem. Simulation parameters are given in Table 1. Two independent 40 GHz radio signals were modulated using a 4-level quadrature amplitude modulation (QAM) followed by modulation by 512 OFDM subcarriers. The purpose of the OFDM modulation is to reduce the multipath fading effect incurred during the transmission through FSO link. The OFDM approach divides the data over a huge number of sub-carriers, which are separated from each other at narrow frequencies.

The OFDM signal was then modulated at 7.5 GHz by using quadrature modulator (QM). This OFDM-QM modulated signal was then fed to a lithium niobate modulator which modulated the two experimental LG modes at 40 GHz. The modulator is assumed to preserve the modal stability of the two channels. The output from the two channels were transmitted over the FSO link.

The link equation for free space optics is modelled by [23]:

$$P_{recieved} = P_{transmitted}\frac{d_R^2}{(d_T+\theta_R)}10^{-\alpha R/10} \tag{2}$$

where d_R defines receiver aperture diameter, d_T is the transmitter aperture diameter, θ is the beam divergence, R is the range and α is the atmospheric attenuation. A Gamma-Gamma distribution is assumed under intensity scintillation [24] to model atmospheric fading. The probability of a given intensity is:

$$P(I) = \frac{2(\alpha\beta^{(\alpha+\beta)2}}{\Gamma(\alpha)\Gamma(\beta)}I^{\frac{\alpha+\beta}{2}-1}K_{\alpha-\beta}\left[2(\alpha\beta I)^{1/2}\right] \tag{3}$$

where

$\alpha = exp\left[\frac{0.49\sigma_R^2}{(1+1.11\sigma_R^{12/5})^{5/6}}\right]-1$, $\beta = exp\left[\frac{0.51\sigma_R^2}{(1+0.69\sigma_R^{12/5})^{5/6}}\right]-1$, α and β are the variances of small and large scale eddies respectively [27], Γ is is the gamma function and $K_{\alpha-\beta}$ is the modified Bessel function of the second kind. The Rytov variance [27] for atmospheric scintillations is assumed:

$$\sigma_R^2 = 1.23C_n^2k^{7/6}z^{11/6} \tag{4}$$

where C_n is the refractive index structure, k is the optical wavenumber and z is the range. Atmospheric turbulence is described by Kolmogorov theory [27]−[29] where the refractive index is expressed as

$$n(\vec{r},t) = n_0 + n_1(\vec{r},t) \tag{5}$$

whereby n_0 is the average index and n_1 is the fluctuation induced by spatial variations of temperature and pressure in the atmosphere. The spatial coherence of the refractive index is governed by [27]−[29]:

$$\rho_{n_1}(\vec{r_1},\vec{r_2}) = E\left[n(\vec{r_1},t)\dot{n}(\vec{r_2},t)\right] \tag{6}$$

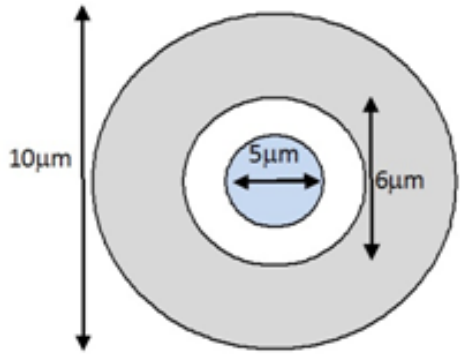

FIG. 4 Spatial photodetector consisting of inner circular aperture for LG00 mode and outer ring aperture for LG10 mode.

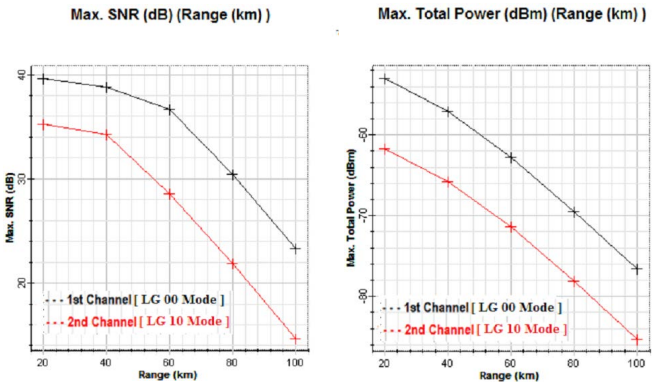

(a) (b)

FIG. 5 Transmission of LG00 and LG10 Channels (a) SNR (b) Total Power.

The wavenumber spectrum $\Phi_n(\vec{k})$ is the spatial Fourier transform of $\rho_{n_1}(\vec{r_1}, \vec{r_2})$ described by [27]–[29]:

$$\Phi_n(\vec{k}) = 0.033 C_n^2 k^{-11/3} \tag{7}$$

where C_n is the refractive index structure given by [27]:

$$C_n^2 = K_0 z^{-1/3} exp\left(-\frac{z}{z_0}\right) \tag{8}$$

where K_0 describes the turbulence strength and z_0 is the effective height of the turbulent atmosphere. C_n^2 varies with the turbulence strength. $C_n^2 = 1 \times 10^{-16}\ \mathrm{m}^{-2/3}$ for weak turbulence and $C_n^2 = 1 \times 10^{-12}\ \mathrm{m}^{-2/3}$ for strong turbulence. The combined signal was then transported over the FSO link and post-amplified using a semiconductor optical amplifier (SOA) with an injection current of 0.5 A. The SOA is modelled to amplify both modes equally. Fraunhoffer diffraction is considered for calculating the wavefield across the (x, y) receiving plane [30]:

$$U(x,y) = \frac{exp(jkz)exp\left(\frac{jk}{2z}\left(x^2+y^2\right)\right)}{j\lambda z} \times \cdots \int\int_{-\infty}^{\infty} U(\epsilon,\eta) exp\left[-j\frac{2\pi}{\lambda z}(x\epsilon + y\eta)\right] d\epsilon d\eta \tag{9}$$

where $U(\epsilon, \eta)$ is the wavefield generated across the transmitting a plane from the spatial light modulator, pinhole and three lenses. z is the free-space distance.

The demultiplexing at the reeiver was simulated in OptiSysytem. The modes were demultiplexed using a spatial

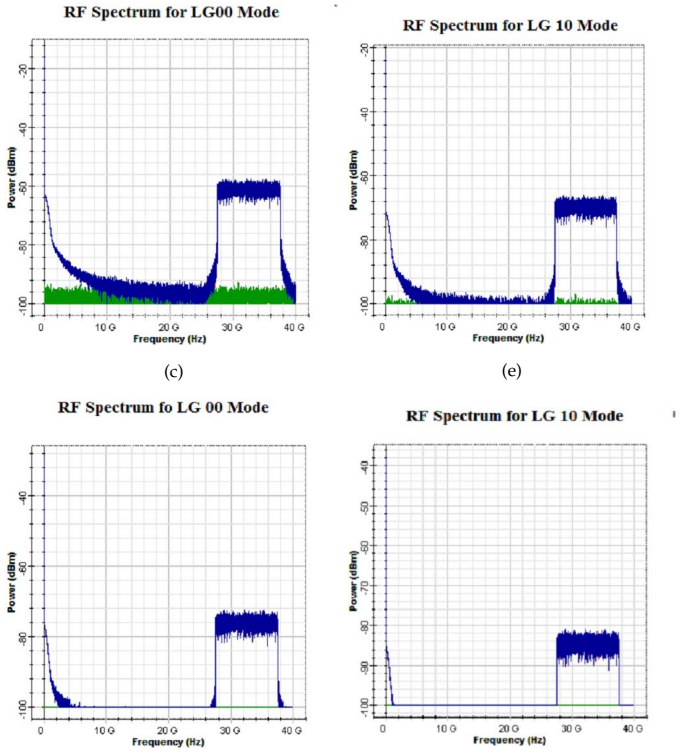

(c) (e)

(d) (f)

FIG. 6 RF spectrum (a) LG00 at 60 km (b) LG00 at 100 km (c) LG10 at 60 km (d) LG10 at 100 km.

photodetector wherein an inner circular aperture of 5 cm was used to extract the LG00 mode and an outer ring aperture of 10 cm was used to extract the LG10 mode. The spatial photodetector is shown in Figure 4. The received power between the two apertures were adjusted such that the intensities on both the circular and outer apertures were equal. A 40 GHz was applied after the photodetector using a mixer in order to recover the SCM signal. Finally the output signal after the mixer was fed to the OFDM demodulator followed by the QM demodulator in order to recover the original data.

3 RESULTS & DISCUSSION

The results from the simulation of the signal propagation through free-space are reported in this section. The two OFDM-Ro-FSO channels are transported over the free space link under clear weather conditions.

It is shown in Figure 5(a) that the value of SNR at the receiver for LG00 channel is 39.56 dB, 36.64 dB and 23.35 dB for an FSO link of 20 km, 60 km and 100 km respectively whereas for LG10, the SNR is 35.21 dB, 28.57 dB and 14.70 dB for an FSO link of 20 km, 60 km and 100 km respectively. From Figure 3(b), the total power received at the receiver is 53.12 dBm, -62.96 dBm and -76.65 dBm for an FSO link of 20 km, 60 km and 100 km respectively whereas for LG10 mode, the total power is -61.67 dBm, -71.42 dBm and -85.62 dBm for an FSO link of 20 km, 60 km and 100 km. This shows that under clear weather conditions the proposed Ro-FSO system will prolong to 90 km with the acceptable SNR and received power.

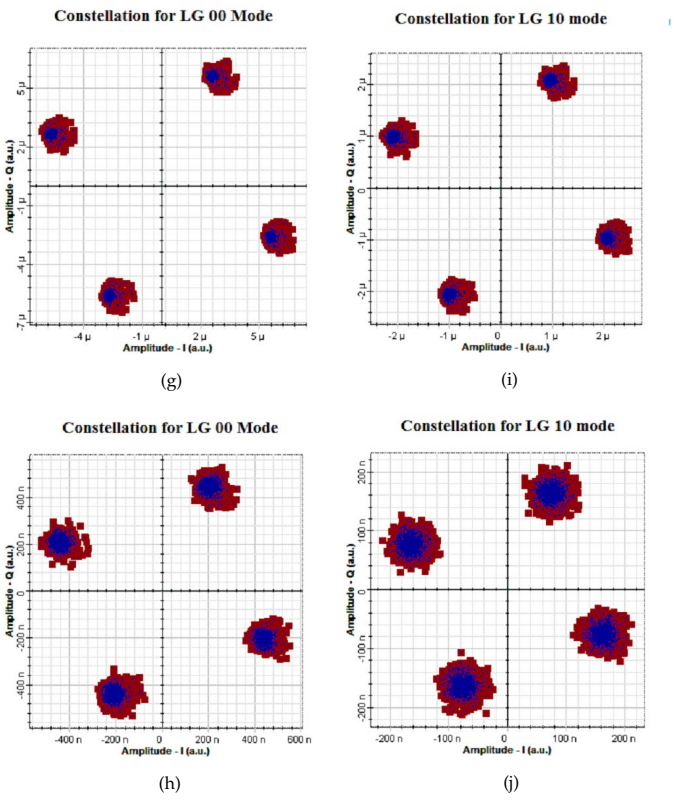

FIG. 7 Constellations Diagram (a) LG00 at 40 km (b) LG00 at 100 km (c) LG10 at 40 km (d) LG10 at 100 km.

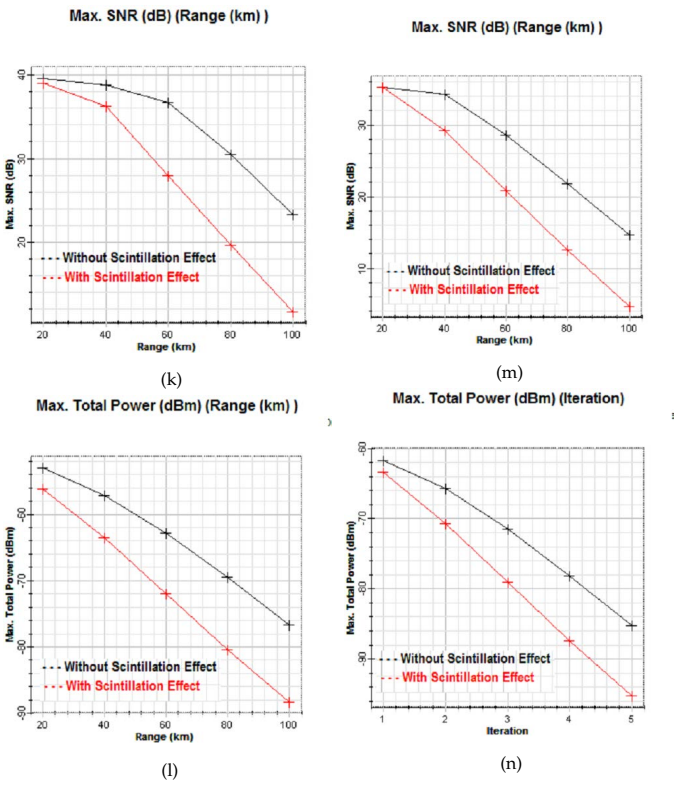

FIG. 8 Under strong turbulences (a) SNR for LG00 (b) Total Received Power for LG00 (c) SNR for LG10 (d) Total Received Power for LG10.

The RF spectrum received in Figure 6 indicates that the RF power degrades as the transmission link increases. Also, more power is received in the LG00 mode compared to the LG10 mode regardless of the distance. This is due to the transformation of the LG10 mode beam profile into a more Gaussian-like distribution whereas the beam profile of LG00 changes less with distance.

Figure 7 reveals the constellation diagrams of the proposed Ro-FSO transmission system under clear weather conditions which indicates that for both the channels the constellation is more precise at 40 km but as the link distance is increased up to a span of 100 km, the noise spectrum increases which makes the constellation distorted. Also, the constellation for the LG00 mode is clearer than the constellation for the LG10 mode regardless of the distance. This is the result of more power collected by LG00 as compared to LG10 due to higher shape distortion in LG10 with distance.

The effect of scintillations for the system is also calculated in Figure 8. Degradations of 13.24 dB in SNR and -12.56 dBm in total received power are reported for a FSO length of 100 km for a LG00 channel under high turbulences in the form of scintillations as compared to the LG10 channel for which degradations of 10.22 dB in SNR and -10.12 dBm in received power are reported at the same FSO length. This indicates that the proposed Ro-FSO system will prolong to 60 km under the effect of strong turbulences with acceptable SNR and received power.

4 CONCLUSION

Two optical LG modes, LG00 and LG10 were multiplexed for transmitting 40 GHz radio QAM-OFDM signals through free-space at a data rate of 20 Gbps for long haul communication. At the receiver, LG00 outperforms LG10 for signal retrieval in terms of the received power and signal constellation regardless of the distance. The achievable distance is 90km under clear weather condition. When scintillation is considered, the achievable distance is 65 km.

5 ACKNOWLEDGMENTS

This work is supported by the Fulbright Foundation of the United States Department of States and Universiti Utara Malaysia.

References

[1] *Facts and Figures* (International Telecommunication Union, 2013).

[2] H. Al-Raweshidy, and S. Komaki, *Radio over fiber technologies for mobile communications networks* (Artech House, Norwood, 2002).

[3] H. A. Willebrand, and S. G. Baksheesh, *Free Space Optics: Enabling Optical Connectivity in Todays Networks* (Sams Publishing, Indianapolis, 2002).

[4] L. C. Andrews, L. P. Ronald, and H. Y. Cynthia, *Laser beam scintillation with applications* (Spie Press Belliongham, Washington, 2001).

[5] H. H. Refai, J. S. Sluss Jr, and H. R. Hazem, "The transmission of multiple RF signals in free-space optics using wavelength division multiplexing," Proc. SPIE **5793**, 1–8 (2005).

[6] A. Bekkali, K. Kazaura, K. Wakamori, T. Suzuki, M. Matsumoto, T. Higashino, et al., "Performance evaluation of an advanced

DWDM RoFSO system for transmitting multiple RF signals," IEICE T. Fund. Electr. **92**, 2697–2705 (2009).

[7] D. R. Kolev, K. Wakamori, and M. Matsumoto, "Transmission Analysis of OFDM-Based Services Over Line-of-Sight Indoor Infrared Laser Wireless Links," J. Lightwave Technol. **30**, 3727–2735 (2012).

[8] A. Amphawan, "Binary encoded computer generated holograms for temporal phase shifting," Opt. Express **19**, 23085–23096 (2011).

[9] A. Amphawan, "Binary spatial amplitude modulation of continuous transverse modal electric field using a single lens for mode selectivity in multimode fiber," J. Mod. Optic. **59**, 460–469 (2012).

[10] S. Randel, R. Ryf, A. Sierra, P. J. Winzer, A. H. Gnauck, C. A. bolle, R. J. Essiambre, et al., "Space-division multiplexing over 10 km of three-mode fiber using coherent $6\times$ 6 MIMO processing," in *proceedings to Optical Fiber Communication Conference and Exposition (OFC/NFOEC), 2011 and the National Fiber Optic Engineers Conference*, 1–3 (IEEE, Los Angeles, 2011).

[11] A. Amphawan, and O. Dominic, "Modal decomposition of output field for holographic mode field generation in a multimode fiber channel," in *proceedings to Photonics (ICP), 2010 International Conference* (IEEE, Langkawi, 2010).

[12] A. Amphawan, V. Mishrab, K. Nisaran, and B. Nedniyomc "Real-time holographic backlighting positioning sensor for enhanced power coupling efficiency into selective launches in multimode fiber," J. Mod. Optic. **59**, 1745–1752 (2012).

[13] A. Amphawan, N. Benjaporn, and M. A. S. Nashwan, "Selective excitation of LP01 mode in multimode fiber using solid-core photonic crystal fiber," J. Mod. Optic. ahead-of-print, 1–9 (2014).

[14] Y. Jung, R. Chen, R. Ismaeel, G. Brambilla, S. U. Alam, I. P. Giles, and D. J. Richardson, "Dual mode fused optical fiber couplers suitable for mode division multiplexed transmission," Opt. Express **21**, 24326–24331 (2013).

[15] Y. Ren, H. Huang G. Xie, N. Ahmed, Y Yan, B. I. Erkmen, N. Chandrasekaran, et al., "Atmospheric turbulence effects on the performance of a free space optical link employing orbital angular momentum multiplexing," Opt. Lett. **38**, 4062–4065 (2013).

[16] J. Wang, J. Y. Yang, I. M. Fazal, N. Ahmed, Y. Yan, H. Huang, Y. Ren, et al., "Terabit free-space data transmission employing orbital angular momentum multiplexing," Nat. Photonics **6**, 488–496 (2012).

[17] H. Huang, G. Xie, Y. Yan, N. Ahmed, Y. Ren, Y. Yue, D. Rogawski, et al., "100 Tbit/s free-space data link enabled by three-dimensional multiplexing of orbital angular momentum, polarization, and wavelength," Opt. Lett. **39**, 197–200 (2014).

[18] Y. Chen, F. Wang, C. Zhao, and Y. Cai, "Experimental demonstration of a Laguerre-Gaussian correlated Schell-model vortex beam," Opt. Express **22**, 5826–5838 (2014).

[19] I. M. Fazal, N. Ahmed, J. Wang, J. Y. Yang, Y. Yan, B. Shamee, H. Huang, et al. "2 Tbit/s free-space data transmission on two orthogonal orbital-angular-momentum beams each carrying 25 WDM channels," Opt. Lett. **37**, 4753–4755 (2012).

[20] T. Su, R. P. Scott, S. S. Djordjevic, N. K. Fontaine, D. J. Geisler, X. Cai, and S. J. B. Yoo, "Demonstration of free space coherent optical communication using integrated silicon photonic orbital angular momentum devices," Opt. Express **20**, 9396–9402 (2012).

[21] P. Polynkin, A. Peleg, L. Klein, T. Rhoadarmer, and J. Moloney, "Optimized multiemitter beams for free-space optical communications through turbulent atmosphere," Opt. Lett. **32** 885–887 (2007).

[22] J. Cang, P. Xiu, and X. Liu, "Propagation of Laguerre-Gaussian and Bessel-Gaussian Schell-model beams through paraxial optical systems in turbulent atmosphere," Opt. Laser Technol. **54**, 35–41 (2013).

[23] R. Chen, L. Liu, S. Zhu, G. Wu, F. Wang, and Y. Cai, "Statistical properties of a Laguerre-Gaussian Schell-model beam in turbulent atmosphere," Opt. Express **22**, 1871–1883 (2014).

[24] L. Pan, C. Ding, and H. Wang, "Diffraction of cosine-Gaussian-correlated Schell-model beams," Opt. Express **22**, 11670–11679 (2014).

[25] A. Amphawan, and W. A. Alabdalleh, "Simulation of properties of the transverse modal electric field of an infinite parabolic multimode fiber," Microw. Opt. Techn. Let. **54**, 1362–1365 (2012).

[26] A. Amphawan, "Holographic mode-selective launch for bandwidth enhancement in multimode fiber," Opt. Express **19**, 9056–9065 (2011) .

[27] L. C. Andrews, and R. L. Phillips, *Laser Beam Propagation Through Random Media* (2nd edition, SPIE Press Book, Bellingham WA, 2005).

[28] M. Born, and E. Wolf, *Principles of Optics* (6th ed., Pergamon Press Canada Ltd., Ontario, 1980).

[29] J. W. Goodman, *Statistical Optics* (Wiley, New York, 1985).

[30] J. Goodman, *Introduction to Fourier Optics* (3rd Edition, Roberts and Company Publishers, Greenwood Village CO, 2004).